Available online at www.sciencedirect.com

ScienceDirect

Ceramics International 39 (2013) 8789–8795

CERAMICS INTERNATIONAL

www.elsevier.com/locate/ceramint

Silver-modified TiO_2 nanorods with enhanced photocatalytic activity in visible light region

Hui Liu*, Xiaonan Dong, Congyue Duan, Xing Su, Zhenfeng Zhu

School of Materials Science and Engineering, Shaanxi University of Science and Technology, Xi'an 710021, PR China

Received 4 March 2013; received in revised form 17 April 2013; accepted 18 April 2013
Available online 28 April 2013

Abstract

Silver-modified TiO_2 nanorods (SMTN) have been synthesized via controlled hydrolysis of tetrabutyltitanate (TBOT) in ethanol and immersion method by using $AgNO_3$ as an Ag source. The physical and chemical properties of SMTN were studied by XRD, SEM, TEM, and UV–vis diffuse reflectance spectra (DRS). The photocatalytic activity of the as-prepared products was evaluated by photocatalytic decolorization of Rhodamine B (Rh B) aqueous solution at ambient temperature under visible light irradiation. The experimental results reveal that the TiO_2 nanorods, which are well dispersed and uniform, attached large numbers of silver nanoparticles on the surface, and the major crystalline phase of TiO_2 is anatase. The photocatalytic activity research shows that the SMTN exhibit an enhanced photocatalytic activity in visible light region compared with that of pure TiO_2 nanorods and commercial TiO_2 (P25).

Keywords: SMTN; SPR; Photocatalytic activity

1. Introduction

One-dimensional oxide semiconductor photocatalysts are one of the most promising materials for environmental remediation due to their unique chemical, physical, thermodynamic and transport properties [1,2]. Among various one-dimensional oxide semiconductor photocatalysts, TiO_2 nanorods have gained more and more attention because of their enhanced properties, cheap, easy acceptance, high specific surface area, and wide applications in waste water purification [3,4], water splitting to create hydrogen [5], solar energy cells [6,7], etc. Although with those unique advantages as a photocatalyst, the inherent weaknesses of the TiO_2 such as the high recombination rate of photo-generated electron–hole pairs and the need for UV radiation to excite electron–hole pairs due to its large band gap (3.2 eV for the anatase phase and 3.0 eV for the rutile phase), limited its broad use in technological applications [8,9]. Recently, many efforts have been attempted to enhance the charge carriers separation efficiency and promote the response and light absorption in the visible region by tuning of the band gap of TiO_2-based photocatalysts. These studies include doping with metal or nonmetal elements [8,10–12], coupling with semiconductors with narrow band gap [13,14], and loading noble metals [7,15–17]. Among these techniques, considerable research has focused on preparation of silver modified TiO_2 photocatalysts due to their superior interfacial charge transfer processes in catalytic reaction [18,19].

To synthesize the silver modified TiO_2 nanorods, various methods, such as the photoreductive method [20], electrochemical deposition method [21] have been used, which processes seemed to be complicated and needed to accurately rationalize several current and potential parameters. Here, we reported a simple and directed deposited method in which the silver-modified TiO_2 nanorods (SMTN) were prepared via controlled hydrolysis of TBOT (tetrabutyltitanate) in ethanol by using $AgNO_3$ as an Ag source and consequent calcination process. On one hand, Ag acted as traps of the photo-generated electrons because of the Schottky barrier on the Ag–TiO_2 interface, thus promoting the separation of photo-generated electrons and holes [9,16]. On the other hand, the as-prepared

*Corresponding author. Fax: +86 29 86177018.
E-mail address: liuhui@sust.edu.cn (H. Liu).

0272-8842/$ - see front matter
http://dx.doi.org/10.1016/j.ceramint.2013.04.066

SMTN could obtain remarkable response and light absorption in visible light region due to the SPR effect caused by the silver nanoparticles [22,23], all of which could largely accelerate the photocatalytic reaction.

2. Experimental

2.1. Materials

All chemicals were analytical grade without further purification. TBOT (tetrabutyltitanate, A. R.) was purchased from Beijing Chemical Regent Co., China. Ethanol (≥99.5%, A. R.) was obtained from Xi'an Chemical Reagent Co., China. KCl (Potassium chloride, A. R.) was obtained from Jinbei Chemical Reagent Co., Ltd., China. $AgNO_3$ (silver nitrate, A. R.) was purchased Guanghua Chemical Reagent Co., Ltd., China.

2.2. Preparation of monodispersed TiO_2 nanorods

TiO_2 nanorods precursor were prepared by controlled hydrolysis of TBOT in ethanol. In a typical experiment, an ethanol volume of 300 mL was mixed with 1.0 mL of aqueous salt solution (KCl, 0.4 mM), after stirring for 20 min, desired amounts of TBOT were added to the mixture and then stirred for about 10 min at a dry atmosphere. Having discontinued stirring for a few hours, the reactions were finished and the white powders were collected by centrifugation and rinsed sequentially with ethanol and water for several times, respectively.

2.3. Preparation of silver nanoparticles modified TiO_2 nanorods

Briefly, 0.1 g as-prepared TiO_2 nanorods were dispersed into 50 mL ethanol and sonicated for 20 min, then a desired amount of $AgNO_3$ solution (the concentration of 1.0 g/L) was added to the solution with continuous stirring and the solvent was evaporated at 80 °C for designed hours. At this point, the heating process was stopped and the suspension was stirred until it cooled to room temperature. The precipitates were collected and then calcinated in air at 500 °C for 2 h to obtain the silver modified TiO_2 nanorods, which were marked as SMTN. To make a comparison, the sample of pure TiO_2 nanorods was also prepared. The preparation process of the pure TiO_2 nanorods was same as the above experimental Section 2.2. Differently, the hydrolysis products were direct calcinated in air at 500 °C for 2 h, which were marked as PT (pure TiO_2 nanorods).

2.4. Characterization

XRD patterns were recorded on a Rigaku D/max 2200 pc diffractometer using Cu Kα radiation of wavelength $\lambda = 0.15418$ nm at 40 kV and 40 mA. FE-SEM (field-emission scanning electron microscope) analysis was performed on a Hitachi S-4800 & Hiroba EDX electron microscopy. TEM images were conducted on a JEM 2010 transmission electron microscope operated at 200 kV. UV–visible absorbance spectra were obtained for the dry-pressed disk samples with a UV–visible spectrophotometer (Lambda-950, PerkinElmer Corporation, American). $BaSO_4$ was used as a reflectance experiment.

2.5. Measurements of photocatalytic activities

The photocatalytic activity of the samples was evaluated in terms of the degradation of Rhodamine B (Rh B) solution. In general, for each test, we carefully prepared 160 mL Rh B solution (the concentration of Rh B 10 mg/L) previously, then the as-prepared Rh B solution was equally transferred into eight quartz photoreactors, which ensured that each quartz tube contained 20 mL Rh B and 20 mg photocatalyst in eight all quartz photoreactors, respectively. The mixture was sonicated for 20 min and stirred for 60 min in the dark in order to reach the adsorption–desorption equilibrium. A 500 W tungsten halogen lamp equipped with a UV cutoff filter ($\lambda > 420$ nm) was used as a visible light source surrounded by a water-cooling quartz jacket to cool the lamp, and ambient temperature was maintained during the photocatalytic reaction. After the photocatalytic reaction, 10 mL of solution was taken and centrifuged. After removing the sediment (photocatalyst particles), the supernatant was used to analyze. The concentration of the residual Rh B was analyzed by checking the absorbance at 553 nm with a UV–vis spectrophotometer.

3. Results and discussion

3.1. XRD patterns

Fig. 1 displays the XRD patterns of the as-synthesized samples. As shown in curve a, the x-ray diffraction peaks at the 2θ values of 25.41°, 37.61°, 48.31°, 54.21° and 62.71° corresponding to the anatase (101), (004), (200), (211) and (204) crystal planes, respectively. These results confirmed that the synthesized materials were TiO_2 of anatase structure with high crystallization and all the diffraction peaks agreed well

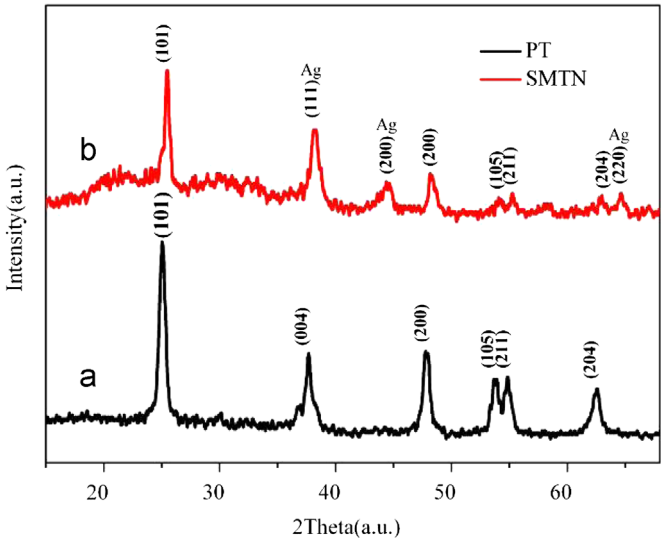

Fig. 1. XRD patterns of TiO_2-based nanorods after calcination: (a) PT and (b) SMTN.

with the reported JCPDS data (Card no. 21-1272). Three apparent diffraction peaks for silver species (38.1°, 44.2°, 64.4°) were observed in curve b, corresponding to the diffraction of (111), (200), (220) planes of face-centered cubic (fcc) silver (JCPDS card no. 04-0783, $a=0.408$ nm) [15]. Besides, as shown in curve b, all the peaks shifted from their positions observed for PT (curve a), which also confirmed that the silver species were transferred into hybrid system successfully [24].

3.2. SEM image

Fig. 2 shows the typical SEM images of the as-prepared PT and SMTN. Seen from Fig. 2a, the calcined sample of PT, which was well dispersed and uniform, was composed of large amounts of fairly uniform TiO_2 nanorods with the diameter of about 50–150 nm. As for the sample of SMTN, the silver-modified TiO_2 nanorods showed comparatively rough surface, which attached large numbers of bright silver grains (Fig. 2b, c). To some extent, based on this kind of Ag-loading process, the SMTN could obtain easy and sufficient contact with Rh B so as to accelerate photocatalytic reaction in visible light region [9,25]. Besides, obviously seen from Fig. 2d, the EDS results revealed Ag elemental peaks, which also confirmed the presence of silver element in the hybrid system. Therefore, on one hand, the sample of SMTN could take advantage of Ag nanoparticles to act as traps of the photo-generated electrons in order to promote the separation of photo-generated electrons and holes. On the other hand, the as-prepared SMTN could obtain remarkable response and light absorption in visible light region because of the SPR effect caused by the silver nanoparticles [22,23,26], so the co-operation of which could largely enhance the photocatalytic efficiency of the samples.

3.3. TEM image

Fig. 3 depicts the morphology of the as-prepared silver-modified TiO_2 nanorods. It could be seen that the SMTN revealed a fairly uniform and narrow size distribution with the

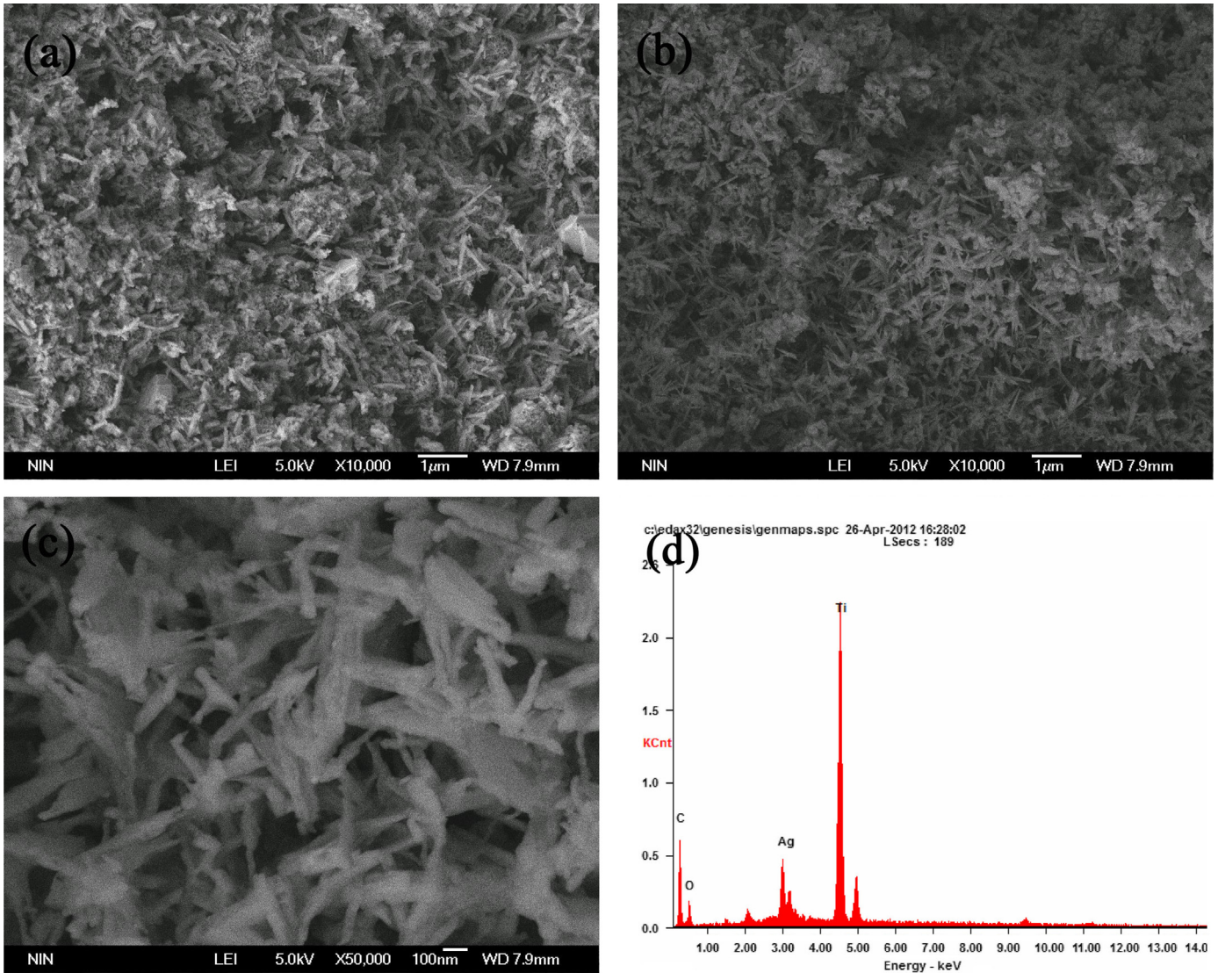

Fig. 2. SEM images of as-prepared TiO_2-based nanorods after calcination: (a) PT, (b) SMTN, (c) higher magnification image of SMTN, and (d) EDS image of SMTN.

diameters of about 50–150 nm (Fig. 3a). The HRTEM images exhibited that the SMTN showed one-dimensional structure and its surface attached lots of bright silver nanoparticles with the diameter of about 5–15 nm (Fig. 3b,c). For one thing, Ag nanoparticles acted as traps of the photo-generated electrons to enhance the separation efficiency of photo-induced charge carriers. For another, SMTN could also obtain remarkable response and light absorption in the visible light region because of the SPR effect caused by the silver nanoparticles so as to accelerate the photocatalytic reaction. As seen in Fig. 3d, the as-prepared SMTN presented the clear lattice fringes owing to its excellent crystallization. In addition, the planes of (200), (111) and (101) were assigned to 3C-silver and anatase TiO_2 respectively [27], which also confirmed that silver and anatase TiO_2 species were all introduced into the hybrid system successfully.

3.4. UV–vis absorption spectra

Fig. 4 shows the UV–vis absorption spectra of PT (a) and SMTN (b) after calcinations, respectively. Obviously, the absorption intensity corresponding to SMTN was lower than that of PT in ultraviolet light region, which was mainly owing to the essential property of semiconductor modified by silver species (curve a) [28]. In comparison, we observed that the response and photo-absorption of PT and SMTN in visible light region were different from that in visible light region. The SMTN exhibited a much continuous and stronger absorption band than that of PT at the range of 400–800 nm, which could be attributed to the surface plasmon resonance of silver nanoparticles [29]. Therefore, firstly we considered that Ag could act as traps of photo-generated electrons to accelerate the separation of electrons and holes, and then we synthesized silver-modified TiO_2 semiconductor nanorods via a simple method. Finally we decorated pure TiO_2 semiconductor nanorods by using $AgNO_3$ as an Ag source to prepare a newly SMTN, which combined the properties of semiconductor and noble metal. When semiconductor contacted with noble metal, Ag could act as traps of photo-generated electrons so as to promote separation of photo-generated electron–hole pairs. Besides, the as-prepared SMTN photocatalyst could obtain

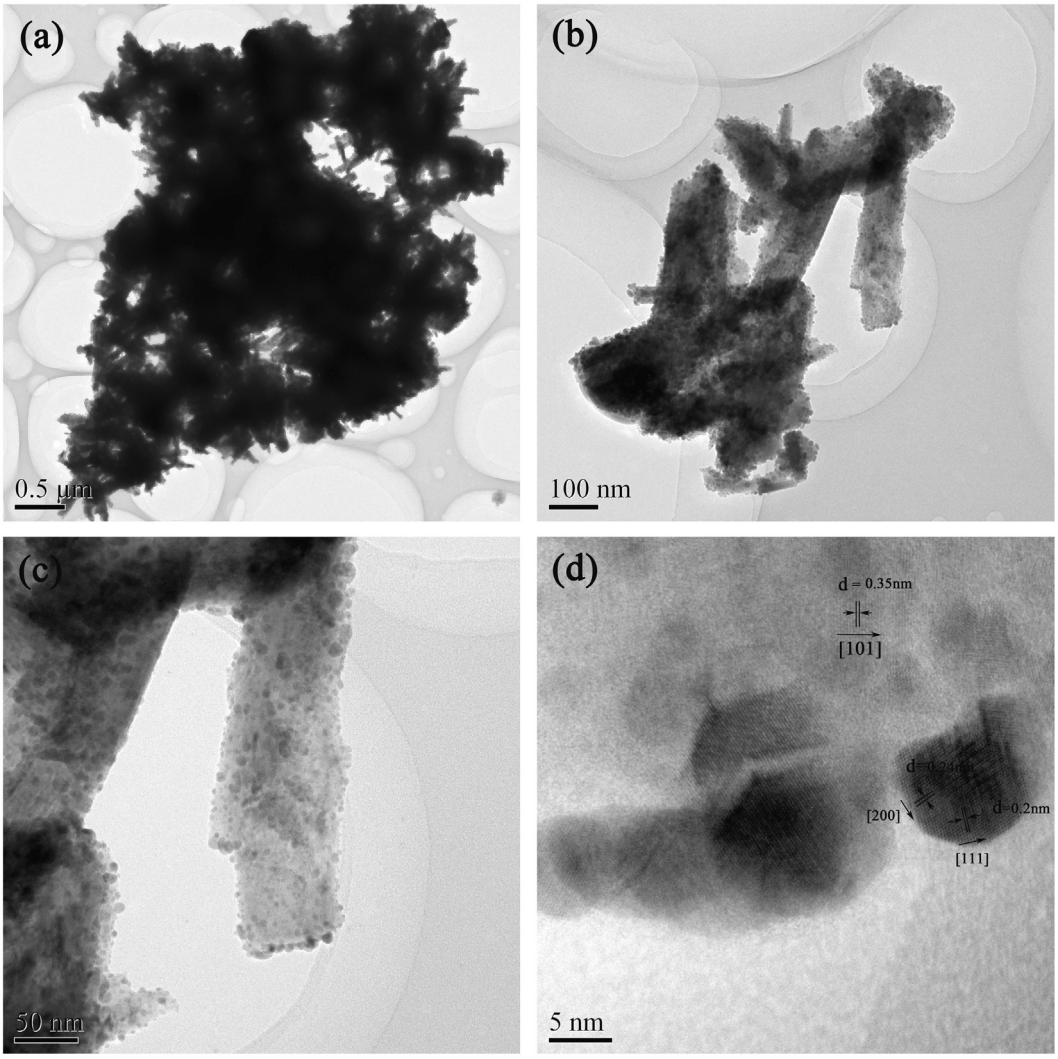

Fig. 3. TEM image of as-prepared TiO_2-based nanorods after calcination, (a) SMTN, (b) HRTEM image of SMTN, (c) HRTEM image of SMTN and (d) HRTEM image of SMTN.

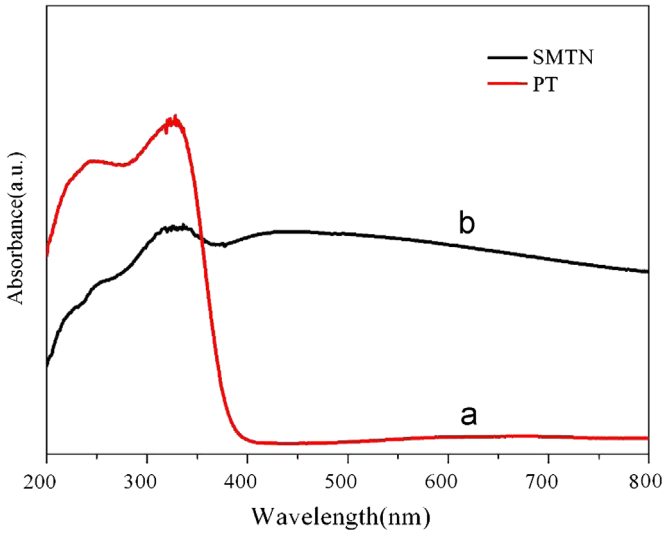

Fig. 4. UV-vis absorption spectra of TiO_2-based nanorods after calcinations: (a) PT and (b) SMTN.

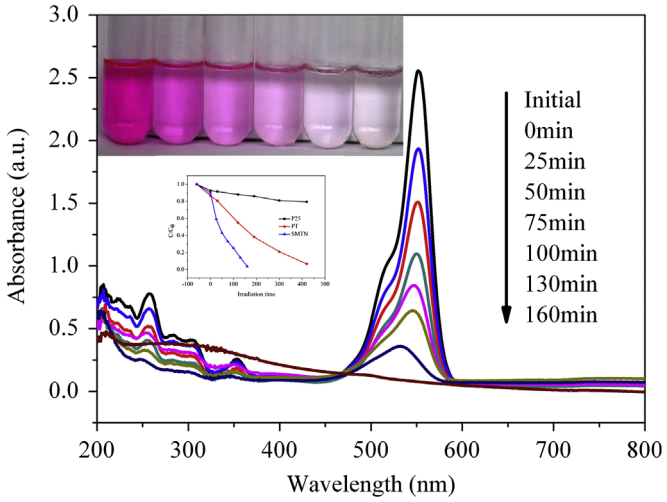

Fig. 5. Photocatalytic degradation of 10 mg/L rhodamine B in the SMTN aqueous suspensions under visible light irradiation. The inset in Fig. 5 gives the comparison of photocatalytic degradation curves of 10 mg/L rhodamine B in the P25, PT, and SMTN aqueous suspensions under visible light irradiation. (For interpretation of the references to color in this figure, the reader is referred to the web version of this article.)

superior response and light-absorption in visible light region because of the SPR effect of silver nanoparticles. Therefore, the newly SMTN photocatalyst could make full use of solar energy as much as possible, which is favorable to the enhancing of photocatalytic activity of TiO_2 in application of the waste water purification.

3.5. Photodegradation activity

Fig. 5 shows the photocatalytic activity of the as-prepared SMTN for the degradation of Rhodamine B (the concentration 10 mg/L) in aqueous solution under visible light irradiation. At the beginning of photocatalytic reaction, the organic waste material (Rh B) adsorbed on the surface of TiO_2 nanorods can be oxidized by the photo-generated holes on valence band, while electronic acceptors (O_2) can receive electrons from the balanced Fermi level so as to promote the photocatalytic activity. As seen in Fig. 5, the photodegradation results revealed that the characteristic absorption band of the Rh B around 553 nm decreased quickly and showed a slight blue shift with the increasing of irradiation time, which ascribed to the N-deethylation of dye during irradiation [30]. Besides, the color of the solution changed from red to colorless in the whole of photocatalytic reaction under visible light irradiation (shown as the inset image in Fig. 5). The inset in Fig. 5 gives the photocatalytic degradation curves of 10 mg/L Rh B of the as-prepared PT, SMTN, and commercial P25 under visible light irradiation, respectively. It is obvious that the samples exhibited diversity of degradation efficiency of Rh B in the photocatalytic reaction. It could be found that the degradation rate showed a similar trend as that of the light absorption intensity in visible region (PT < SMTN) (Fig. 4). In addition, the absorption volume of all samples is similar to the UV–vis absorption trend (P25 < SMTN < PT) at the stage of absorption balance process (Inset in Fig. 5), as the effective specific surface area that could be used for absorbed organic dye got decreased after silver loaded on the surface of TiO_2 nanorods. Based on the co-operation of trap levels and SPR effect, the newly SMTN could show an enhanced photocatalytic activity than that of P25 and PT. The sample of PT could gather abundant organic dye on the surface of semiconductor so that it could exhibit a better photocatalytic activity than P25 in the final time [9]. In a word, we have successfully synthesized the newly SMTN photocatalyst, which was expected to be promising candidate as effective photocatalyst applied to waste water purification.

3.6. Mechanism on enhancement of photocatalytic activity

The enhanced photocatalytic performance of the SMTN can be explained by assuming the formation of trap levels and SPR effect, and a possible proposed energy band structure of SMTN is elucidated schematically in Scheme 1. Silver and TiO_2 semiconductor have different work function. The former has a higher work function (Fm) than the latter (Fs). When the two materials are contacted with each other, the metal-semiconductor hybrid can increase the absorption and light response in visible region because of the formation of defect level [31–33]. During the photocatalytic process, the photo-generated electrons can migrate from TiO_2 nanorods to silver until the two Fermi level positions are aligned. When the newly SMTN hybrid structure is radiated by visible light, due to the trap levels and the influence of the SPR effect in the metal-semiconductor hybrid structure, the photo-generated electrons easily transfer from the conductive band of TiO_2 nanorods to that of silver nanoparticles, which act as traps level of electrons, thus largely promoting the separation efficiency of photo-generated electron–hole pairs. Then, the photo-generated electrons react with absorbed O_2 and H_2O on the surface of the hybrid structural photocatalyst and produce superoxide radical anions, such as $\bullet O_2^-$. The photo-generated

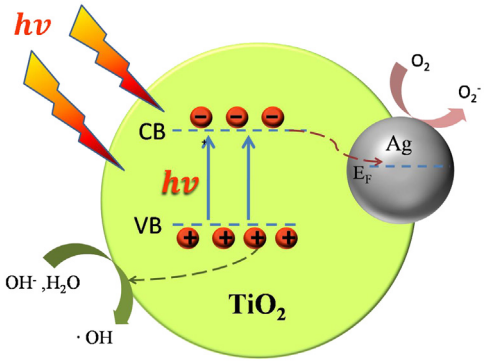

Scheme 1. Proposed photocatalytic mechanism of silver modified TiO_2 nanorods.

holes can be trapped by H_2O and absorbed OH^- to further produce •OH species. Therefore, the photo-generated electron–hole pairs could be separated efficiently on the SMTN interface to participate further in a chemical reaction and produced powerful superoxide radical as well as oxidizing agent ($\bullet O_2^-$, •OH) that degradated the organic dyes under visible light irradiation.

4. Conclusions

In conclusion, silver-modified TiO_2 nanorods (SMTN) have been synthesized via controlled hydrolysis of TBOT (tetrabutyltitanate) in ethanol and immersion method by using $AgNO_3$ as an Ag source. The experimental results reveal that silver-modified TiO_2 nanorods, which surface attached large numbers of silver nanoparticles with the diameter of about 5–15 nm, are distributed uniformly and the major crystalline phase of TiO_2 is anatase. On one hand, the formation of traps level could accelerate electrons to move from semiconductor to silver so as to enhance the separation efficiency of photo-generated electron-hole pairs and generate more active oxygen species so as to cause the oxidative decomposition of Rh B. On the other hand, the newly SMTN could obtain remarkable response and light-absorption due to the SPR effect of silver nanoparticles, all of which could greatly promote the photocatalytic activity of the sample. The silver-modified TiO_2 nanorods were expected to be promising candidates as effective photocatalysts in waste water purification.

Acknowledgments

We acknowledge financially supported from the National Science Foundation of China (51272147), the Doctoral Research Start-up Fund of Shaanxi University of Science and Technology (BJ10-12), Special Fund from Shaanxi Provincial Department of Education (12JK0467) and the Graduate Innovation Found of Shaanxi University of Science and Technology.

Reference

[1] H. Tong, S. Ouyang, Y.P. Bi, N. Umezawa, M. Oshikiri, L.H. Ye, Nano-photocatalytic materials: possibilities and challenges, Advanced Materials 24 (2012) 229–251.

[2] C.S. Guo, J. Xua, Y. Hea, Y. Zhang, Y.Q. Wang, Photodegradation of rhodamine B and methyl orange over one-dimensional TiO_2 catalysts under simulated solar irradiation, Applied Surface Science 257 (2011) 3798–3803.

[3] J.C. Liu, L. Liu, H.W. Bai, Y.J. Wang, D.D. Sun, Gram-scale production of graphene oxide-TiO_2 nanorod composites: towards high-activity photocatalytic materials, Applied Catalysis B: Environmental 106 (2011) 76–82.

[4] D.V. Dudina, S.B. Zlobin, N.V. Bulina, A.L. Bychkov, V.N. Korolyuk, V.Y. Ulianitsky, O.I. Lomovsky, Detonation spraying of TiO_2-2.5 vol% Ag powders in a reducing atmosphere, Journal of the European Ceramic Society 32 (2012) 815–821.

[5] A. Kubacka, M. Fernandez-García, G. Colon, Advanced nanoarchitectures for solar photocatalytic applications, Chemical Reviews 112 (2012) 1555–1614.

[6] T.W. Zeng, C.C. Ho, Y.C. Tu, G.Y. Tu, L.Y. Wang, W.F. Su, Correlating interface heterostructure, charge recombination, and device efficiency of poly(3-hexyl thiophene)/TiO_2 nanorod solar cell, Langmuir 27 (2011) 15255–15260.

[7] S.H. Kang, S.H. Choi, M.S. Kang, J.Y. Kim, H.S. Kim, T. Hyeon, Y. E. Sung, Nanorod-based dye-sensitized solar cells with improved charge collection efficiency, Advanced Materials 20 (2008) 54–58.

[8] X.Z. Wei, H.J. Wang, G.F. Zhu, J.Y. Chen, L.P. Zhu, Iron-doped TiO_2 nanotubes with high photocatalytic activity under visible light synthesized by an ultrasonic-assisted sol-hydrothermal method, Ceramics International 39 (2013) 4009–4016.

[9] H. Liu, X.N. Dong, G.J. Li, X. Su, Z.F. Zhu, Synthesis of C, Ag co-modified TiO_2 photocatalyst and its application in waste water purification, Applied Surface Science 271 (2013) 276–283.

[10] F. Dong, H.Q. Wang, Z.B. Wu, One-step "Green" synthetic approach for mesoporous C-Doped titanium dioxide with efficient visible light photocatalytic activity, Journal of Physical Chemistry C 113 (2009) 16717–16723.

[11] Z.A. Xiong, X.S. Zhao, Nitrogen-Doped Titanate-Anatase Core−Shell Nanobelts with exposed {101} anatase facets and enhanced visible light photocatalytic activity, Journal of the American Chemical Society 134 (2012) 5754–5757.

[12] W.L. Xu, P.K. Jain, B.J. Beberwyck, A.P. Alivisatos, Probing redox photocatalysis of trapped electrons and holes on single Sb-doped titania nanorod surfaces, Journal of the American Chemical Society 134 (2012) 3946–3949.

[13] W. Smith, A. Wolcott, R.C. Fitzmorris, J.Z. Zhang, Y.P. Zhao, Quasi-core-shell TiO_2/WO_3 and WO_3/TiO_2 nanorod arrays fabricated by glancing angle deposition for solar water splitting, Journal of Materials Chemistry 21 (2011) 10792–10800.

[14] D.S. Wang, Y.H. Wang, X.Y. Li, Q.Z. Luo, J. An, J.X. Yue, Sunlight photocatalytic activity of polypyrrole-TiO_2 nanocomposites prepared by 'in situ' method, Catalysis Communications 9 (2008) 1162–1166.

[15] V. Subramanian, E.E. Wolf, P.V. Kamat, Catalysis with TiO_2/Gold nanocomposites. Effect of metal particle size on the fermi level equilibration, Journal of the American Chemical Society 126 (2004) 4943–4950.

[16] W. Zhao, L.L. Feng, R. Yang, J. Zheng, X.G. Li, Synthesis, characterization, and photocatalytic properties of Ag modified hollow SiO_2/TiO_2 hybrid microspheres, Applied Catalysis B: Environmental 103 (2011) 181–189.

[17] S.C. Hsu, W.P. Liao, W.H. Lin, J.J. Wu, Modulation of photocarrier dynamics in Indoline Dye-Modified TiO_2 nanorod array/P3HT hybrid solar cell with 4-tert-butylpridine, Journal of Physical Chemistry C 116 (2012) 25721–25726.

[18] M.K. Seery, R. George, P. Floris, S.C. Pillai, Silver doped titanium dioxide nanomaterials for enhanced visible light photocatalysis, Journal of Photochemistry and Photobiology A: Chemistry 189 (2007) 258–263.

[19] H.H. Mohamed, R. Dillert, D.W. Bahnemann, Growth and reactivity of silver nanoparticles on the surface of TiO_2: a stopped-flow study, Journal of Physical Chemistry C 115 (2011) 12163–12172.

[20] E.Y. Bae, W.Y. Choi, Highly enhanced photoreductive degradation of perchlorinated compounds on Dye-Sensitized Metal metal/TiO_2 under visible light, Environmental Science and Technology 37 (2003) 147–152.

[21] S.C. Chan, M.A. Barteau, Preparation of highly uniform Ag/TiO_2 and Au/TiO_2 supported nanoparticle catalysts by photodeposition, Langmuir 21 (2005) 5588–5595.
[22] M. Jakob, H. Levanon, P.V. Kamat, Charge distribution between UV-irradiated TiO_2 and gold nanoparticles: determination of shift in the Fermi level, Nano Letters 3 (2003) 353–358.
[23] S. Sakthivel, M.V. Shankar, M. Palanichamy, B. Arabindoo, D. W. Bahnemann, V. Murugesan, Enhancement of photocatalytic activity by metal deposition: characterisation and photonic efficiency of Pt, Au and Pd deposited on TiO_2 catalyst, Water Research 38 (2004) 3001–3008.
[24] C Suwanchawalit, S. Wongnawa, P. Sriprang, P. Meanha, Enhancement of the photocatalytic performance of Ag-modified TiO_2 photocatalyst under visible light, Ceramics International 38 (2012) 5201–5207.
[25] D. Sarkar, C.K. Ghosh, S. Mukherjee, K.K. Chattopadhyay, Three dimensional Ag_2O/TiO_2 type-II (p–n) nanoheterojunctions for superior photocatalytic activity, ACS Applied Materials and Interfaces 5 (2013) 331–337.
[26] A.B. Haugen, I. Kumakiri, C. Simon, M.A. Einarsrud, TiO_2, TiO_2/Ag and TiO_2/Au photocatalysts prepared by spray pyrolysis, Journal of the European Ceramic Society 31 (2011) 291–298.
[27] Y.N. Xia, Y.J. Xiong, B. Lim, S.E. Skrabalak, Shape controlled synthesis of metal nanocrystals: simple chemistry meets complex physics, Angewandte Chemie International Edition 47 (2008) 2–46.
[28] S. Ramya, S.D. Ruth Nithila, R.P. George, D.N. Gopala Krishna, C. Thinaharan, U. Kamachi Mudali, Antibacterial studies on Eu–Ag codoped TiO_2 surfaces, Ceramics International 39 (2013) 1695–1705.
[29] Y.H. Zhang, Z.R. Tang, X.Z. Fu, Y.J. Xu, Nanocomposite of Ag–AgBr–TiO_2 as a photoactive and durable catalyst for degradation of volatile organic compounds in the gas phase, Applied Catalysis B 106 (2011) 445–452.
[30] J.M. Du, J.L. Zhang, Z.M. Liu, B.X. Han, T. Jiang, Y. Huang, Controlled synthesis of Ag/TiO_2 core–shell nanowires with smooth and bristled surfaces via a one-step solution route, Langmuir 22 (2006) 1307–1312.
[31] X.X. Zou, R. Silva, X.X. Huang, J.F. Al-Sharab, T. Asefa, A self-cleaning porous TiO_2–Ag core-shell nanocomposite material for surface-enhanced Raman scattering, Chemical Communications 49 (2013) 382–384.
[32] S.L. Wang, H.H. Qian, Y. Hu, W. Dai, Y.J. Zhong, J.F. Chen, X. Hu, Facile one-pot synthesis of uniform TiO_2–Ag hybrid hollow spheres with enhanced photocatalytic activity, Dalton Transactions 42 (2013) 1122–1128.
[33] L.M. Jiang, G. Zhou, J. Mi, Z.Y. Wu, Fabrication of visible-light-driven one-dimensional anatase TiO_2/Ag heterojunction plasmonic photocatalyst, Catalysis Communications 24 (2012) 48–51.